

## P 1.60 ON THE CORRELATION OF BOUNDARY LAYER WIND MAXIMUMS AND VERTICAL VELOCITIES ASSOCIATED WITH AN MM5 SIMULATION OF SUPERTYPHOON HERB (1996)

David B. Radell\*<sup>1</sup>, Chun-Chieh Wu<sup>2</sup>, and Chia-Bo Chang<sup>3</sup>

<sup>1</sup> Department of Geosciences, University of Nebraska-Lincoln, Lincoln, NE, USA

<sup>2</sup> Department of Atmospheric Sciences, National Taiwan University, Taipei, Taiwan

<sup>3</sup> Atmospheric Science Group, Texas Tech University, Lubbock, TX, USA

### 1. INTRODUCTION

Numerous modeling projects have undertaken the task of analyzing the interaction between a landfalling tropical cyclone and a significant terrain feature. Mesoscale variations in tropical cyclone (TC) strength, track and structure have led to significant forecasting problems in these regions. Contributing to this problem further is the lack of meteorological observing platforms in the mountainous regions most affected by landfalling TC's. For example, Chang (1982), Bender et al (1985), and Wu and Kuo (1999) all examined the orographic influence on the structure, path, environment and intensity of numerically simulated tropical cyclones traversing Taiwan.

Severe downslope wind events have been studied from both the theoretical and numerical prospective using local hydraulic theory (LHT, eg. Smith, 1985; Gutman, 1991). However, further investigation is needed on the combination of severe downsloping winds in the vicinity of a landfalling TC. Property owners inhabiting these regions would benefit from improved prediction of these occurrences to better protect their interests. Further, TC track variation and strength may be significantly affected by mesoscale features generated on the eastern side of Taiwan. In this study, we seek to gain further insight into intense boundary layer winds produced as a cyclone passes over Taiwan. The effects Taiwan's topography on the TC environment is also studied through an MM5 simulation of Supertyphoon Herb (1996). Boundary layer wind maximums and their relation to regions of negative vertical motion are analyzed. Several questions arise as to the mechanism responsible for the generation of these mesoscale downdrafts and subsequent downsloping winds that develop along the southeastern edge of Taiwan. One result of these downdrafts is the generation of a pressure trough along the eastern edge of the Central Mountain Range (CMR). A hypothesis for the responsible mechanism and implications on the TC environment are presented.

### 2. BACKGROUND

Supertyphoon Herb was a devastating, category five TC that made landfall on the mountainous island of Taiwan in July 1996.

---

*Corresponding author address:* David B. Radell, Meteorology/Climatology Program, 214 Bessey Hall, University of Nebraska-Lincoln, Lincoln, NE, 68508.  
Email: dradell@foehn.unl.edu

Taiwan is often chosen as a representative land mass for the examination of a TC-orographic interaction due to its unique geographic makeup, lack of observation network over the Pacific Ocean and the frequency of typhoons impacting the island (average of 3.7 per year over a 20 year period, Wu et al., 1999). As displayed in Figure 1, the CMR follows the major axis of the island and reaches elevations of greater than 3 km at its peaks. Two topographic areas of interest within the CMR arise in this case, centered around the "northern" (Hsuehshan) and "southern" (Yü Shan) peak areas. The Penn State University/National Center for Atmospheric Research Mesoscale Model 5 (MM5) Version 3, with a fine horizontal resolution of 6.67 km and 23  $\sigma$  (or terrain-following) levels in the vertical was used for the simulation.

### 3. ANALYSIS

Figure 2 depicts a horizontal plot of the model surface ( $\sigma = 1$ ) wind speeds and streamlines for 1000 UTC, 31 July 1996. Isotach contour intervals are in 5  $\text{ms}^{-1}$  intervals (beginning at 30  $\text{ms}^{-1}$ ). At this time, the westernmost flow associated with the TC begins to make landfall. Two distinct features are immediately revealed. First, as exemplified by the nearly closed streamline to the north, the eye of the typhoon is evident just onshore Taiwan. Its position is along the extreme northeastern coast of the island, away from any significant terrain features. Secondly, as compared to the CMR from Figure 1, maximum surface winds (solid isotachs) are found immediately east/southeast of the two major peaks (elevation ~3 km) introduced earlier. In comparison with previous model studies, we define the "lee" side as the eastern region of the CMR, as the flow associated with Herb is westerly during the time frame of interest. Wind speeds of greater than 30  $\text{ms}^{-1}$  are contoured on the lee side to the southeast of both the northern and southern peaks. Maximum values for this time period exceed 50  $\text{ms}^{-1}$ . Of interest is the perpendicular nature of the streamlines to the major axis of the CMR. The streamlines exhibit a more westerly component (as compared to prior times) and are oriented almost normal to the highest topography. As the streamlines associated with the typhoon rotate in a cyclonic fashion about the island with time and became more normal to the highest peaks, surface wind speeds generally increase on the lee slopes.

To gain a better idea of the moisture as well as the downward motion associated with the surface wind maxima, Figure 3 displays the total accumulated rainfall (solid, in 200 mm intervals) at 1000 UTC with

isotachs (dashed, in  $1 \text{ ms}^{-1}$  intervals) for downward motion. Convective precipitation was not an available plotting option in this instance, the logical choice when analyzing vertical motions in an orographic scenario. Note that the precipitation maxima are located due upstream of the strongest regions of downward motion. At 0800 UTC (not shown), the sinking motion exhibits similar characteristics to that of the surface wind speed, having an orientation nearly parallel to the topography. Maximum values of sinking motion ( $\sim 3 \text{ ms}^{-1}$ ) for this time correlate quite well with the regions of maximum wind speed. For this time period wind speeds of greater than  $40 \text{ ms}^{-1}$  match up well with the  $3 \text{ ms}^{-1}$  sinking air. By 1000 UTC, lee side sinking air motions have increased in magnitude as has the windward total rainfall amount. The spatial distribution of both have remained relatively similar to the 0800 UTC case. The largest sinking motion values now reach  $4 \text{ ms}^{-1}$  and correlate quite well with the  $50 \text{ ms}^{-1}$  surface winds as shown in Figure 3.

The vertical structure of the wind speed (solid) and sinking motion (dashed) is examined through the depth of the model atmosphere for this time period and is exhibited in Figure 4. Contour intervals for both variables are as in previous figures. The cross section is oriented east-west and taken through the southern CMR peak (refer to inset) at a latitude of approximately  $22.5^\circ\text{N}$ . It is important to note that the cross section is *not* taken through the typhoon itself, but rather well to its south in the area of greatest surface wind speeds. This image exemplifies the vertical coherence of both parameters. Of interest is the maximum value for each at about the 3 km height level (just over the peaks) and the downward extension of these maximum values toward the surface. Clearly, the maximum values for wind speed correspond very well with sinking motion. At 0800 UTC (not shown), maximum winds ( $> 50 \text{ ms}^{-1}$ ) and downward motion ( $> 5 \text{ ms}^{-1}$ ) are vertically aligned. The same holds true two hours later at 1000 UTC, with an increase in both variables. Maximum winds are now greater than  $60 \text{ ms}^{-1}$  from about 3 km to the surface while downward motion values are now at approximately  $6 \text{ ms}^{-1}$ . The mesoscale downdrafts appear to originate near the 650 hPa level based on Figure 4. In a spatial sense, the correlation seems to hold throughout the depth of the lower atmosphere, particularly from the surface to the 600 hPa level.

We next seek to identify the mechanism(s) responsible for the generation of these boundary layer wind maximums as well as possible implications to the TC track. As the cyclone approaches Taiwan, a westerly shift in its path is noted at approximately 0400 UTC, some 6 hours prior to landfall and 4 hours prior to the next track shift to the southwest. Figure 5 displays a vertical cross section of equivalent potential temperature (denoted  $\theta_e$ ) for 2200 UTC July 30, about 12 hours before landfall. To the west of the CMR, lower  $\theta_e$  air is found at mid levels and just above the highest peaks, indicative of the relatively drier air aloft. This dry air is a byproduct of the orographically induced precipitation

found just to the west. To the east of the CMR higher  $\theta_e$  values exist, ranging from 360 K to 364 K. A plot of the relative humidity (RH, not shown) over the island at this time shows rather dry air (RH values of 40%-50%) to the east just over the significant terrain features and is coincident with the most significant downward motion. This indicates that the downsloping air is very dry and warms adiabatically upon descent. This eastern slope "foehn" effect has been well documented in previous research (eg. Chang, 1993) in association with TCs traversing Taiwan. The westward propagation and mixing down of this low  $\theta_e$  air over the higher  $\theta_e$  air on the lee side acts to initiate the mesoscale downdrafts, ultimately resulting in the observed surface lee wind maxima. With only a difference of 14 K between the "moist" and "dry" air from the eastern surface to about 700 mb above the CMR, it would be interesting to study further the minimum vertical gradient required to initiate such phenomena, if it is indeed responsible.

Finally, in relation to the boundary layer wind maxima, we note the development of an eastern (lee) trough at about 0200 UTC as Herb approaches Taiwan. Figure 6 displays this feature, with a plot of sea level pressure at 0600 UTC just before Herb makes landfall. As the TC approaches, the trough deepens. As a result, easterly boundary layer winds increase due to the strengthened east-west oriented pressure gradient force. By 1200 UTC, the trough weakens and the boundary layer winds subside in response. Just after the development of this lee trough, Herb's track shifts from northwest to due west (0400 UTC), until turning to the southwest just before landfall (0800 UTC). At this time, we are unsure as to the effect (if any) that this lee trough has on the propagating TC, other than its development and extinction coincides with these track changes. Future work would perhaps shed additional light on this issue.

#### 4. SUMMARY

As we have shown, just before and during the landfall of a numerically simulated TC, a spatial and temporal correlation is seen between boundary layer maximum winds speeds and downward vertical motion. There is convincing model evidence that an approximate 10:1  $\text{ms}^{-1}$  ratio exists between boundary layer wind maxima and downward motion, respectively. The mixing down of lower  $\theta_e$  air is the likely generation mechanism that initiates these downsloping winds. We have proposed that these downdrafts create a surface pressure trough that causes a strong easterly boundary layer wind to develop along the eastern side of the CMR. Additionally, as the TC approaches Taiwan, its track changes significantly in a short period of time, coincident with the development of a lee pressure trough. Several interesting questions arise from this analysis. First, does the development of the lee pressure trough act to modify the TC's track? Second, are the lee mesoscale downdrafts driven more significantly by thermodynamic or kinematic processes? Clearly, additional research is necessary in this area to

answer these and additional questions about the interactions between a TC and orography.

## 5. ACKNOWLEDGEMENTS

This project was partially supported by the Texas Board of Higher Education Grant ATM-0990004.

## 6. REFERENCES

- Bender, M.A., R. Tuleya and Y. Kurihara, 1985: A numerical study of the effect of a mountain range on a landfalling tropical cyclone. *Mon. Wea. Rev.*, **113**, pp. 567-582.
- Chang, C.-P., and J.M. Chen, 1993: Effects of terrain on the surface structure of typhoons over Taiwan. *Mon. Wea. Rev.*, **121**, pp. 734-752.
- Chang, S., 1982: The orographic effects induced by an island mountain range on propagating tropical cyclones. *Mon. Wea. Rev.*, **110**, pp. 1255-1270.
- Gutman, Lev N., 1991: Downslope windstorms. Part I: effect of air density decrease with height. *J. Atmos. Sci.*, **48**, pp. 2545-2551.
- Smith, Ronald B., 1985: On severe downslope winds. *J. Atmos. Sci.*, **42**, pp. 2597-2603.
- Wu, C.-C. and Y.-H. Kuo, 1999: Typhoons affecting Taiwan: Current understandings and future challenges. *Bull. Amer Meteor. Soc.*, **80**, pp. 67-80.

## 7. FIGURES

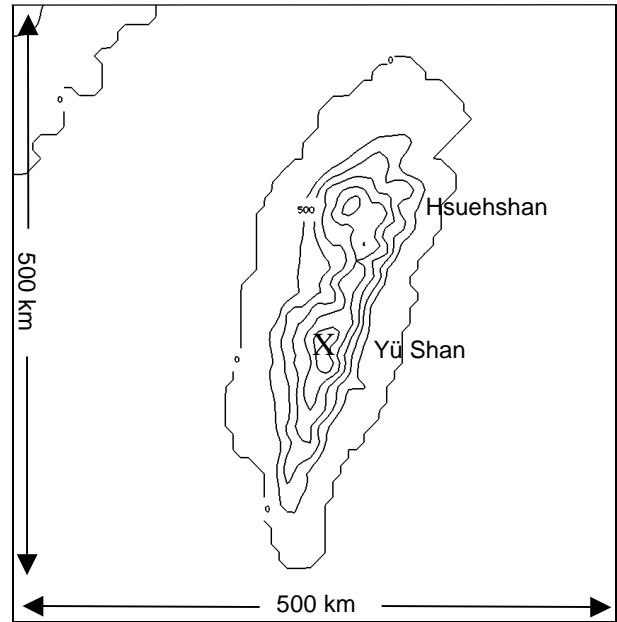


FIGURE 1. Taiwan topography in 500 m intervals. Approximate domain is 500 x 500 km.

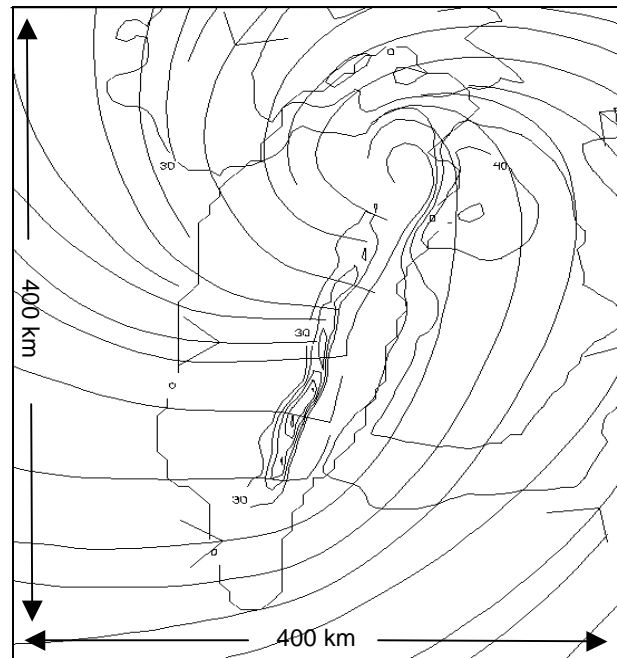


FIGURE 2. Model surface ( $\sigma = 1$ ) streamlines and wind speed ( $5 \text{ ms}^{-1}$  intervals) at 1000 UTC, 31 July 1996.

7. FIGURES CON'T

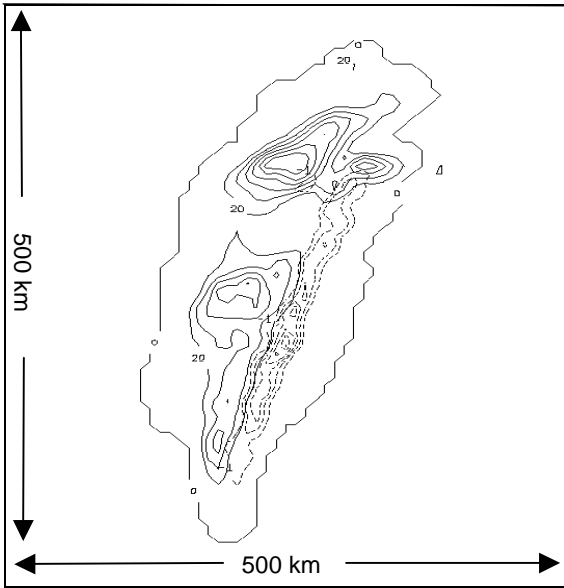


FIGURE 3. Model surface ( $\sigma=1$ ) downward ( $-W$ ) motion ( $1 \text{ ms}^{-1}$  intervals, dashed) and total accumulated rain water (20 mm, solid) at 1000 UTC, 31 July 1996.

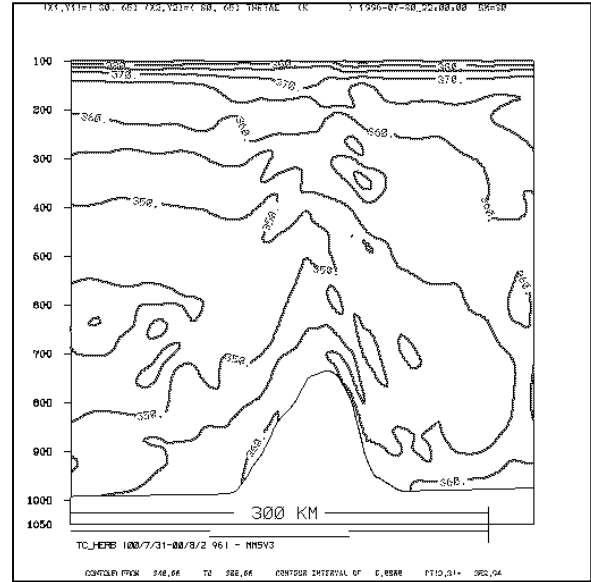


FIGURE 5. Vertical cross section of equivalent potential temperature,  $\theta_e$ , in 5 K intervals. The cross section is taken through the same latitude as in Figure 4, and is valid 2200 UTC 30 July, 1996.

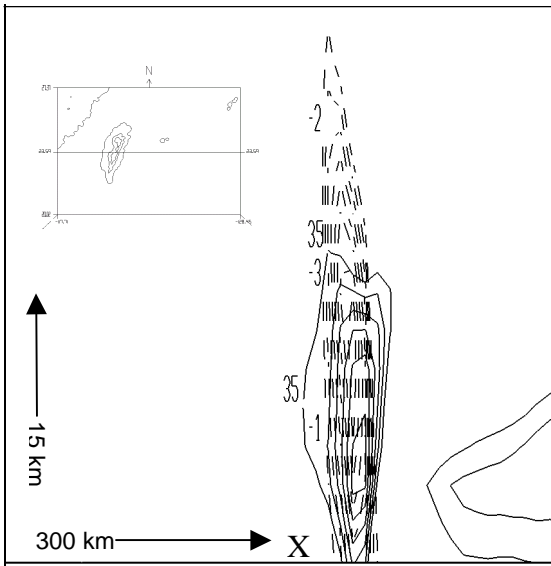


FIGURE 4. Vertical cross section of downward motion (dashed) in  $1 \text{ ms}^{-1}$  intervals and wind speed in  $5 \text{ ms}^{-1}$  intervals beginning at  $35 \text{ ms}^{-1}$ . Inset shows latitude of cross section. Time is 1000 UTC 31 July 1996, and approximate figure dimensions are 300 km by 15 km. The CMR is marked with an 'X'.

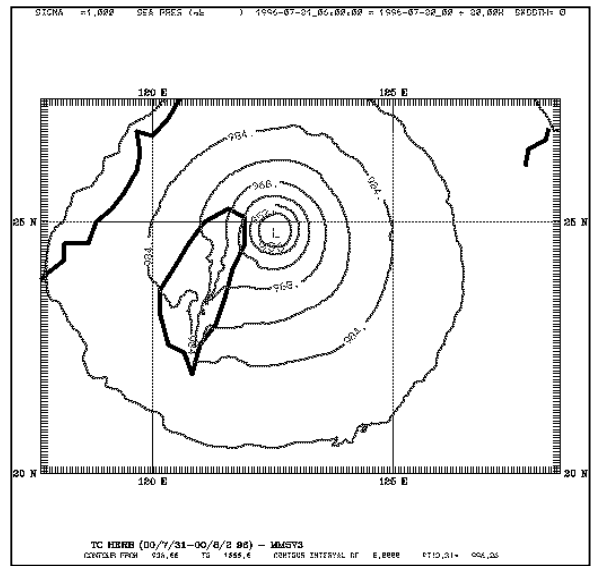


FIGURE 6. Surface ( $\sigma=1$ ) pressure in 8 hPa intervals valid 0600 UTC 31 July, 1996.